Available online at www.sciencedirect.com
SCIENCE DIRECT®
Materials Research Bulletin 40 (2005) 1–11
Materials Research Bulletin
www.elsevier.com/locate/matresbu

Influence of spectator ions on the reactivity of divalent metal salts in molten alkali metal nitrates Morphology of the resulting metal oxides

P. Marote[a,*], C. Matei[b], C. Sigala[c], J.P. Deloume[d]

[a]*UMR Sciences Analytiques 5180, Université Claude Bernard Lyon 1, CPE Bat 308, 43 Bd du 11 novembre 1918, 69122 Villeurbanne Cedex, France*
[b]*Department of Inorganic Chemistry, Politehnica University of Bucharest, 1 Polizu Street, 78126 Bucharest Romania, P.O. Box 12-205, France*
[c]*Laboratoire des Multimatériaux et Interfaces, UMR 5615, Université Claude Bernard Lyon 1, France*
[d]*LACE, UMR 5634, Université Claude Bernard Lyon 1, France*

Received 10 December 2002; received in revised form 27 September 2004; accepted 5 October 2004

Abstract

This work focuses on the investigation of the reaction of alkali metal nitrates ($LiNO_3$, $NaNO_3$ and KNO_3) with divalent metal salts (Cu^{2+}, Ni^{2+} and Zn^{2+}). Thermogravimetric analysis (TGA) was employed to study the kinetics and mechanisms of the above reactions, which led to the formation of the corresponding metal oxides. The reaction temperature was found to depend not only on the alkali metal but also on the metal salt (MCl_2 or $M(NO_3)_2$) involved in the reaction.

SEM observations show that the spectator ions present in the reacting medium have varying degrees of influence on the morphology of the powder; the growth directions, sizes and the homogeneity of their distribution, are modified. KNO_3 generates the most significant differences compared to $LiNO_3$ and $NaNO_3$.

Keywords: A. Oxides; B. Crystal growth; C. Thermogravimetric analysis (TGA); C. Electron microscopy

* Corresponding author. Tel.: +33 04 72 43 1001; fax: +33 04 72 44 8319.
E-mail address: marote@univ-lyon1.fr (P. Marote).

0025-5408/$ – see front matter
doi:10.1016/j.materresbull.2004.10.001

1. Introduction

Molten alkali metal nitrates (AMN) have received much attention during the last decade owing to their potential application as solvents and reaction media [1]. Numerous studies have been carried out using the so-called nitrate eutectics ($1NaNO_3/1KNO_3$) [2,3]. The main advantages of these mixtures include their low melting temperature and their practical interest for alkali nitrate reactions. Despite these reports, the effect of the alkali metal ion requires more careful consideration. Indeed, it is well known that the choice of the alkali metal ion can influence the melting point of the AMN. The choice of the metal ion (M^{n+}) can also modify the Lux-Flood acido-basic equilibrium Eq. (1) [4,5].

$$2ANO_3 \rightleftarrows 2A^+ + 2NO_2 + \frac{1}{2}O_2 + O^{2-} \tag{1}$$

According to Eq. (2) the oxide ion, O^{2-}, readily leads to the formation of metal oxides and therefore M^{n+} has to be considered as a Lux-Flood acid.

$$M^{n+} + \frac{n}{2}O^{2-} \rightarrow MO_{n/2} \tag{2}$$

Clearly, a better understanding of the nature of the metal ion effect on the final product is essential. The metal ion acidity depends on the formal charge and also influences the basicity of the molten salts. Since tetravalent metals [6–8] are considered as strong acids, the difference of basicity between the three AMNs disappears [9]. Therefore, it would be necessary to use metal ions having an acidity of the same order of magnitude as the basicity of AMN to reveal their differences. Ni, Cu and Zn nitrates and chlorides were chosen because of the two plus ($^{2+}$) charge of the cations, and also because they are not able to undergo oxidation in the nitrate medium. Zinc is often compared to the alkaline-earth metals (weak acids); therefore the Zn^{2+} ion will be weakly acid. Nickel and copper ions will therefore also be weak to medium acids.

The aim of this work is to put in light both the influence of the alkali metal ion and the role of the spectator anion of the metal precursor on the morphology of the oxides obtained by reaction in the molten AMN.

2. Experimental

2.1. Materials

The metal precursors $CuCl_2{\cdot}2H_2O$ (Merck, 99%); $Cu(NO_3)_2{\cdot}3H_2O$ (Merck, 99%); $NiCl_2{\cdot}6H_2O$ (Prolabo, 98%); $Ni(NO_3)_2{\cdot}6H_2O$ (Merck, 99%); $ZnCl_2$ (Prolabo, 98%); $Zn(NO_3)_2{\cdot}4H_2O$ (Merck, 98.5%) were used without further purification. The alkali metal nitrates $LiNO_3$ (Aldrich 98%), $NaNO_3$ (Prolabo P.A), and KNO_3 (Prolabo P.A) were dried at 120 °C and stored in an oven at 100 °C before being used.

2.2. Procedure

The reaction for the formation of a metal oxide starting from an anhydrous metal salt is as follows [1,4]:

$$MX_n + nANO_3 \xrightarrow{\text{excess } ANO_3} MO_{n/2} + nAX + nNO_2 + \frac{n}{2}O_2 \quad (3)$$

Neither A^+ nor X^- take a part in the reaction and so they could be omitted (from a strictly chemical point of view). The gaseous compounds evolve from the medium while AX ($X = NO_3^-$, Cl^-) as well as the excess of ANO_3, are soluble in water. The metal oxide is isolated by filtration. The AMNs have been used in excess to provide the liquid phase throughout the experiment. The ratio AMN/metal precursor was 8/1 [10,11]. The progress of the reaction was monitored by following the evolution of mass loss: the gases generated by the reaction. This was performed with a modified Setaram B70 thermobalance with a heating rate of 150 °C/h from room temperature up to 500 °C. The mass of precursor involved corresponded to about 1.5×10^{-4} mol.

The metal oxide used for the characterizations was obtained by reaction in test tubes. About two grams of metal oxide were prepared with the following thermal schedule: ramp from room temperature to 100 °C: 1 h; level out at 100 °C: 1 h; ramp to 450 °C: 3 h and level at 450 °C: 2 h; cooling at the cooling rate of the furnace.

The characterization was performed by X-ray diffraction (XRD) using a D500 Siemens diffractometer located at the Center of Diffraction Henri Lonchambon, Université Lyon1. Microscopy was carried out using a Hitachi S800 Scanning Electronic Microscope at the Centre des Microstrctures, Université Lyon1. The chemical analyses were performed at the Central Service of Analysis, C.N.R.S, in Vernaison, France, using standardized techniques.

3. Results

3.1. Characterizations

The oxides obtained have been characterized by X-ray-diffraction and chemical analysis. For reasons of clarity we will write the origin of the oxide in the form of MO[X–A] where X is the anion of the metal precursor and A is the alkali metal of the nitrate used in the reaction. Therefore, the notation NiO [Cl–K] means that the NiO is obtained by the reaction of $NiCl_2$ with KNO_3.

3.2. X-ray diffraction

For each metal oxide obtained, XRD shows one single phase in agreement with ICDD files 44-1159, 45-0937 and 326-1451 for NiO, CuO and ZnO, respectively. The systematic addition of silicon as the angular position standard allows us to conclude that there is no shift in the d spacings and consequently that no solid solution is formed with the alkali metal ion.

The relative intensities fit the ICDD files for NiO and CuO but not for ZnO. The differences and changes are resumed in Table 1.

The figures in Table 1 show that the alkali metal and the anion play a role in the crystal growth. In addition, the narrow peak widths prove the high degree of crystallisation and the large size of the crystals.

Table 1
Comparison of the relative intensities of the three most intense peaks of the six zinc oxides prepared

Relative intensity of hkl	1 0 0	0 0 2	1 0 1
ICDD ZnO	57	44	100
ZnO [Cl–Li]	100	8	29
ZnO [Cl–Na]	100	15	38
ZnO [Cl–K]	100	34	12
ZnO [NO_3–Li]	9	100	27
ZnO [NO_3–Na	78	100	67
ZnO [NO_3–K]	95	100	53

3.3. Chemical analyses

The results of the chemical analyses of the transition metal oxide products obtained for impurity ions are shown in Table 2. We could observe that the amounts of impurities in all the oxides (Table 2) are small. The atomic alkali metal content varies from a maximum of 4% for $Ni(NO_3)_2$–$LiNO_3$ and a minimum of 0.4% for $Ni(NO_3)_2$–KNO_3. However, the zinc oxide obtained from the $ZnCl_2$ salt, shows a greater impurity content. This difference is evident in the high value of the chlorine fraction present in sodium nitrate. The potassium and chloride content is greater in ZnO than in CuO and NiO, for the oxides obtained in KNO_3. The same observation was made in the two other media, however the differences between the impurity contents in NiO and in CuO are smaller.

3.4. Thermal stability of the precursors

We systematically draw the loss of mass in g mol^{-1} of transition metal ion. This allows direct comparisons on the reactivity of the different salts whatever their molar weight. The thermogravimetric (TG) curves of the thermal decomposition of the six precursors are similar to those described in the literature [11,19]. That is, among the metal nitrates, only $Zn(NO_3)_2{\cdot}4H_2O$ dehydrates immediately at about 270 °C [11–13]. The two others, Cu and Ni, form basic nitrates [11–15], weakly stable at 200 and 240 °C for copper (Fig. 1) and nickel, respectively. The next mass loss leads to the metal oxide, at about

Table 2
Chemical analyses of the impurities in the oxides of Ni, Cu and Zn prepared from different precursors in the different molten media (at%)

Precursors	Product	Medium								
		$LiNO_3$			$NaNO_3$			KNO_3		
		Li	N	Cl	Na	N	Cl	K	N	Cl
$NiCl_2{\cdot}6\ H_2O$	NiO	1.18	0.53	0.85	0.52	0.53	1.23	0.011	0.53	0.61
$Ni(NO_3)_2{\cdot}6\ H_2O$	NiO	3.98	0.69		0.55	1.23		0.003	0.53	
$CuCl_2{\cdot}2\ H_2O$	CuO	0.21	0.56	0.45	0.55	0.56	0.63	0.016	0.56	0.47
$Cu(NO_3)_2{\cdot}3\ H_2O$	CuO	0.28	0.56		0.2	0.56		0.17	0.56	
$ZnCl_2$	ZnO	1.18	0.58	0.92	0.73	0.9	8.01	0.52	0.58	0.92
$Zn(NO_3)_2{\cdot}4\ H_2O$	ZnO	1.18	0.58		0.53	0.58		0.42	0.58	

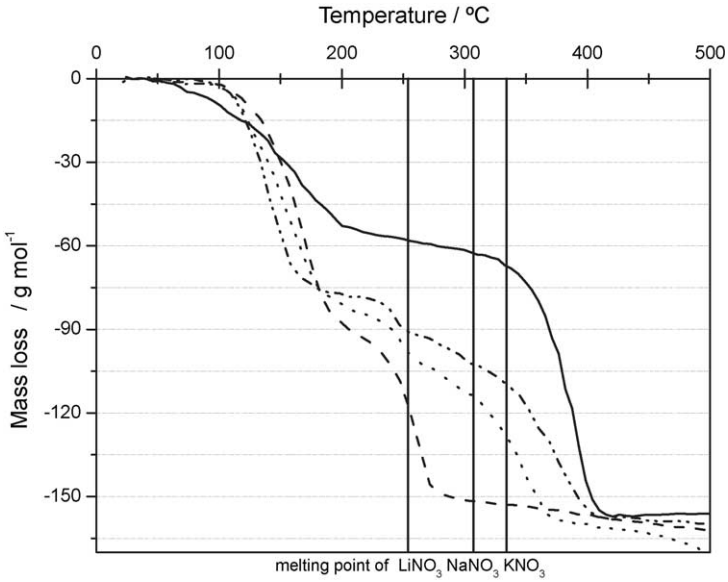

Fig. 1. TGA of $Cu(NO_3)_2{\cdot}3H_2O$, ••••••••••• in $LiNO_3$, — · · — · · in $NaNO_3$, ▬▬▬ in KNO_3, - - - - - precursor alone.

300 °C, with a yield of 100%. Zinc chloride is anhydrous and stable up to 450 °C. $CuCl_2{\cdot}2H_2O$ undergoes a one step dehydration (Fig. 2) ending at 120 °C [16,17]. $NiCl_2{\cdot}6H_2O$ is dehydrated in two steps; the first one (110 °C) leads to $NiCl_2{\cdot}2H_2O$ and the second produces NiO (250 °C) in agreement with the literature [18,19].

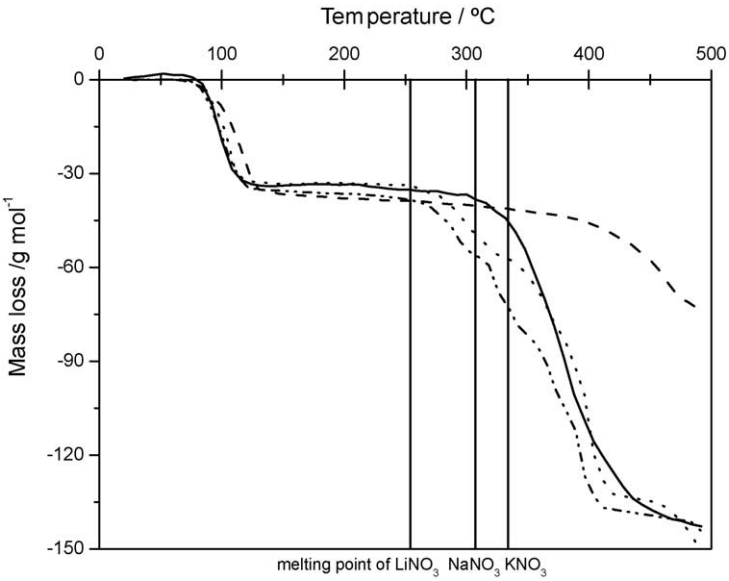

Fig. 2. TGA of $CuCl_2{\cdot}2H_2O$, ••••••••••• in $LiNO_3$, — · · — · · in $NaNO_3$, ▬▬▬ in KNO_3, - - - - - precursor alone

3.5. Reactivity in the molten salts

All the metal precursors except $ZnCl_2$ react in the media with a 100% yield according to the overall, mass loss determined from the general equation:

$$MX_2 \cdot xH_2O + 2ANO_3 \xrightarrow{\text{excess } ANO_3} MO + 2AX + 2NO_2 + \frac{1}{2}O_2 + xH_2O \quad (4)$$

The mass of gas phase produced in the reaction (4) is $\Delta m = 18\ x + 108$ g mol^{-1}M^{2+}.

We have observed three kinds of TGA curves: the first concerns the metal nitrates; the second, the copper and nickel chlorides; and the third, zinc chloride.

3.5.1. Reactivity of the metal nitrates

The reaction of the metal nitrates generally follows the curves shown in the Fig. 1 which represent the reaction of $Cu(NO_3)_2{\cdot}3H_2O$. We observe a modification of the dehydration step, mainly in KNO_3. This salt (the most ionic and the least basic) prevents the formation of the basic nitrate and instead results in the anhydrous $Cu(NO_3)_2$ which reacts at about 300 °C to give CuO. In the other AMN, the TG curve corresponds, for the temperatures below 250 °C, to the decomposition curve of the precursor. The differences observed between 200 and 250 °C could correspond to the stabilization of the intermediate species [$3Cu(NO_3)_2{\cdot}Cu(OH)_2{\cdot}H_2O$] by the nitrates. This has been already described in the literature [11–15]. The formation of this intermediate requires the release of ten H_2O and two HNO_3 which corresponds to $\Delta m = 306/4 = 76.5$ g mol^{-1} in agreement with the observed mass loss (Fig. 1, $NaNO_3$). The stabilization of this species causes an increase in the temperature of formation of the metal oxide (Table 3).

Dehydration of nickel nitrate and zinc nitrate both lead to similar mass loss, whatever the AMN (ca. 75 g mol^{-1} for nickel and 108 g mol^{-1} for the zinc salt). Therefore, the oxide formation curves look very similar too. The temperature of the maximum rate of formation of the metal oxide increases according to the AMN in the order Li, Na and K (Table 3).

Copper nitrate appears to be the least stable of the three metal nitrates whereas zinc nitrate reacts at the highest temperature, which confirms its trend to behave as an alkaline earth metal. It is worth noting that the reaction goes to completion with this zinc salt (vide infra zinc chloride).

3.5.2. Reaction of copper and nickel chlorides

The copper and nickel chlorides (di- and hexahydrate, respectively) undergo dehydration to the anhydrous chlorides, which are stable until relatively high temperatures. Fig. 2 shows that $CuCl_2$ begins to be oxidized by the ambient oxygen at about 400 °C. For this reason the oxide formation

Table 3
Temperature of the maximum rate of reaction of metal oxide formation starting from a metal nitrate in the alkali metal nitrates

Maximum rate temperature (°C)	$Cu(NO_3)_2{\cdot}3H_2O$	$Ni(NO_3)_2{\cdot}6H_2O$	$Zn(NO_3)_2{\cdot}4H_2O$
Precursor only	269	304	323
Precursor in $LiNO_3$	350	354	366
Precursor in $NaNO_3$	376	388	418
Precursor in KNO_3	392	423	441

Table 4
Temperature of the maximum rate of the reaction of formation of a metal oxide starting from a metal chloride in the alkali metal nitrates

Maximum rate temperature (°C)	$CuCl_2$	$NiCl_2$
In $LiNO_3$	390	418
In $NaNO_3$	368	418
In KNO_3	380	439

TG curves start from a well-defined plateau (from 120 °C to about 250 °C) and over a narrow temperature range. The maximum rate temperatures remain similar as shown in Table 4. Moreover, the temperature domain is comparable to the reaction temperature of the respective transition metal nitrate in KNO_3.

3.5.3. Reaction of zinc chloride

Zinc chloride is particularly sensitive to the reaction medium. In every case, the TG curve reaches a plateau; the oxide is not totally formed as the thermal decomposition of the AMN begins to affect the reaction. At 500 °C the mass losses are 138, 109 and 51 g mol^{-1} in Li, Na and KNO_3, respectively. Consequently, the reaction yields (450 °C for 2 h) decrease in the same order: 98, 85 and 70%. These results show the differences in reactivity due to the medium and the metal salt.

In the case of the metal nitrates, the reactive species are present from the beginning. When the precursor is heated alone, it cannot transfer the thermal energy to other entities, therefore the cation and the nitrate ions are directly involved, and so the reaction temperature is low. The presence of the AMN could account for an energy radiator, however the thermal conductivities of the AMN decrease from Li to KNO_3 [20] and the order of the reaction temperatures should be the inverse of the observed one. Complexes can be formed with the nitrate ions of the AMN as shown by Liu et al. [21] and Eweka et al. [2]. These complexes are all the more stable since the medium is less basic and the nitrate ion more symmetric; the temperature of reaction increases from Li to KNO_3.

When the metal chlorides are involved, the nitrate ions have to enter the coordination sphere before reacting. As the stability of the chloro species depends only on the metal and chloride ions the energy required is approximately the same whatever the alkali metal. The reaction temperatures systematically increase, eventually they are close to that for reaction of the metal nitrate in KNO_3. The uncompleted reaction of $ZnCl_2$ related to the total one of $Zn(NO_3)_2$ helps this assumption.

3.6. Scanning electron microscopy

This technique was used to demonstrate relationships occurring between the reactivity and the crystallite morphologies. The space groups of the oxides are different: rhombohedral with a rock salt structure for NiO, monoclinic with a distorted rock salt structure for CuO and hexagonal with a würtzite structure for ZnO. The comparisons are only valid for a single metal with respect to one precursor and one medium; we choose to begin with the lowest symmetry oxide.

Fig. 3 presents the micrographs obtained with CuO. CuO[Cl] forms systematically agglomerates of about 20 μm. The crystallites show different shapes according to the medium, and an irregular growth

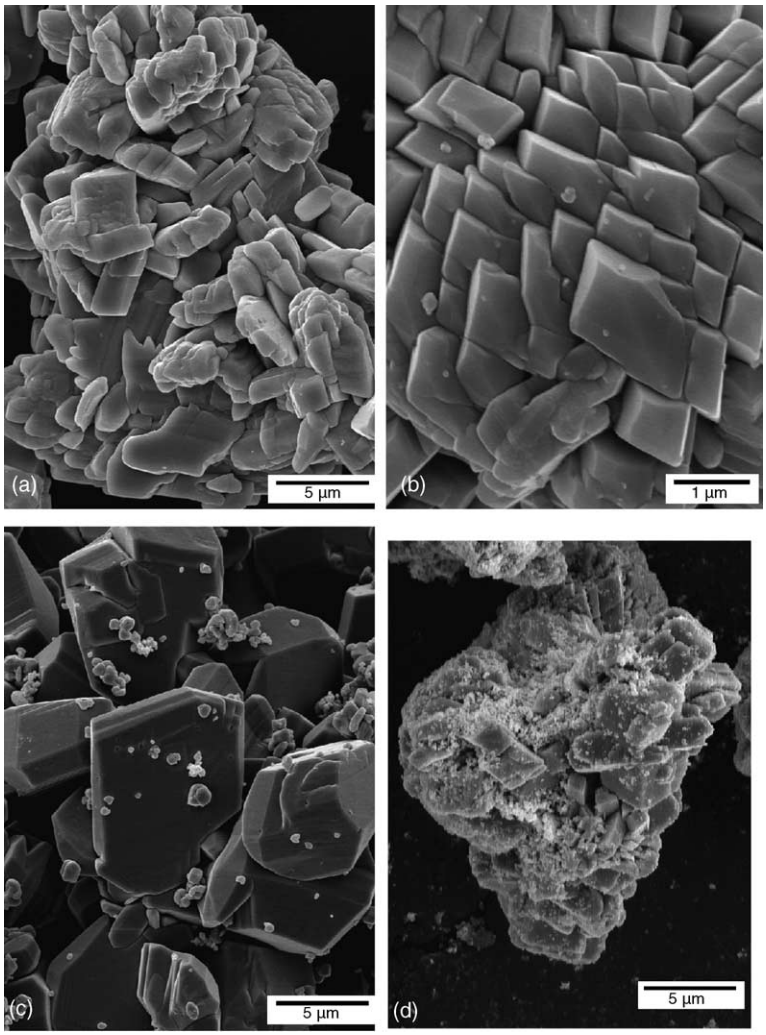

Fig. 3. (a) CuO obtain using $CuCl_2$ in $LiNO_3$, (b) CuO obtain using $CuCl_2$ in $NaNO_3$, (c) CuO obtain using $Cu(NO_3)_2$ in $LiNO_3$ and (d) CuO obtain using $Cu(NO_3)_2$ in KNO_3.

characterizes the reaction in $LiNO_3$ (Fig. 3a). In Na and KNO_3 the crystallites are elongated ($1\ \mu m^2 \times 5\ \mu m$, Fig. 3b), ore over, in relation to this kind of growth, large X cross-shaped crystals (30 μm) can be observed. CuO[Cl, K] differs from CuO[Cl, Na] by the presence of very small crystallites (20 nm) on the surface of the larger ones. In comparison to this, the aggregates formed by CuO[NO_3] look different, probably because the directions of growth are not similar to the previous ones. In $LiNO_3$ (Fig. 3c), the size distribution is quite monomodal, whereas, in both other AMNs, the powders are mixtures of polycrystalline (20 μm) aggregates and small (50nm) crystallites (Fig. 3d). To summarise therefore, the crystal shape of CuO depends on the precursor, and the size and aggregation depend on the medium.

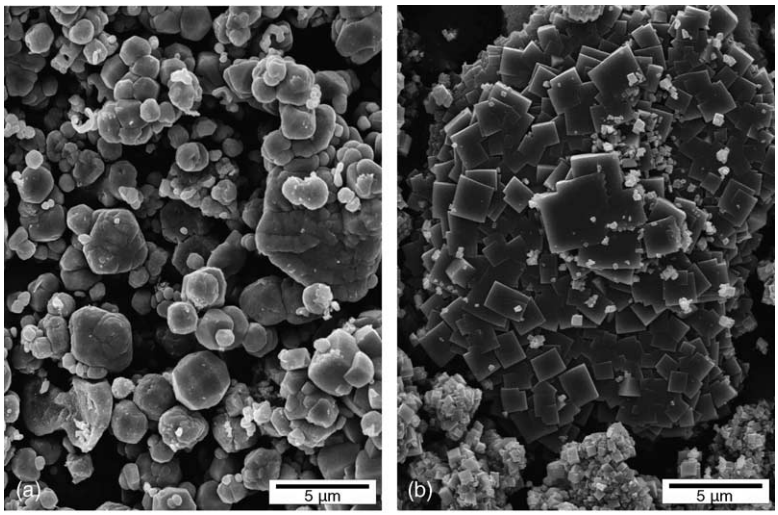

Fig. 4. (a) NiO obtain using $NiCl_2$ in $LiNO_3$ and (b) NiO obtain using $Ni(NO_3)_2$ in KNO_3.

The micrographs of NiO seem on the whole rather similar. NiO[Cl,Li] and NiO[Cl,Na] are comparable. The sizes of the agglomerates are different, but they are constituted from spheroid crystallites (Fig. 4a) whose varies from 500 nm to 2.5 μm. In NiO[Cl,K] the shapes become more angular, cubic shaped aggregates appear. The examination of NiO[NO_3, Li] or NiO[NO_3,Na] shows that the upper limit of the crystal sizes is closer to 1 μm than to 2.5 μm as in the previous oxides. The shapes are less spheroid and more octahedral. NiO[NO_3,K] is different as can be observed in Fig. 4b: large and compact agglomerates of cubes of 1 to 2 μm as well as the same kind of agglomerates of cubes 0.5 μm in size. For this oxide the most significant feature is the difference, which appears when the medium is KNO_3 whatever the precursor.

Most of the micrographs of ZnO show particles of large size, isolated from each other. The solids observed correspond to different crystal growth. According to the structure, the unit part of these building is a thin hexagonal crystallite as shown on Fig. 5a. The nature of the precursor influences growth and agglomeration of the crystallites. With $ZnCl_2$ the trend is a development along the *c* axis, as shown partially on Fig. 5a. Several kinds of solids are observed, most of them with a central hole. The most complete ones obtained in $NaNO_3$ (Fig. 5b), look like a smooth hexagonal tube. Once more, in KNO_3 the trend vanishes and a randomisation of the shapes appears. The ZnO[NO_3] powders have different crystal shapes in $LiNO_3$ and KNO_3. In the first one, the growth and agglomeration lead to large hexagonal plates (>20 μm) like ornaments as shown on Fig. 5c. However, in $NaNO_3$, the plates are hexagonally drilled and needles appear. Finally in KNO_3, only needles are observed, and they are moreover covered with very small crystallites (Fig. 5d). These differences of growth explain the differences observed in the relative intensities of the X-ray diffractograms.

Among the three metal oxides, ZnO[NO_3] shows the most significant changes according to the precursor and the liquid medium, and in general in the case of zinc, we characterize one powder for one medium and one precursor.

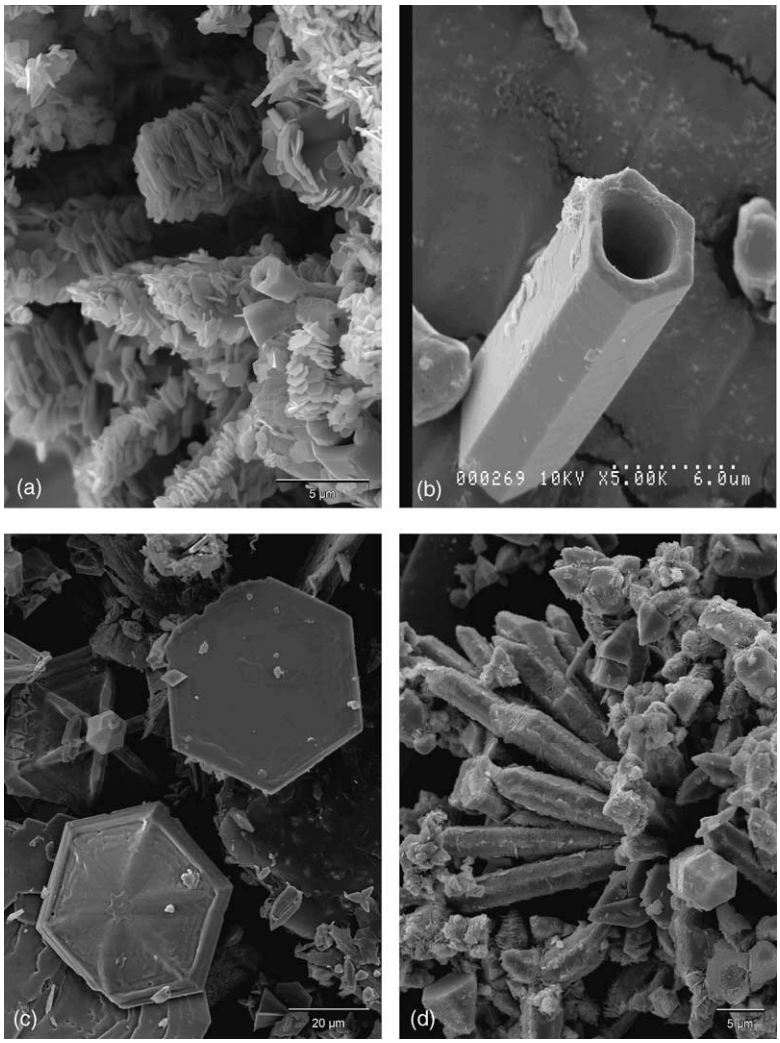

Fig. 5. (a) ZnO obtain using $ZnCl_2$ in $LiNO_3$, (b) ZnO obtain using $ZnCl_2$ in $NaNO_3$, (c) ZnO obtain using $Zn(NO_3)_2$ in $LiNO_3$ and (d) ZnO obtain using $Zn(NO_3)_2$ in KNO_3.

4. Conclusion

TG analyses have shown the differences in the reactivity of the metal precursors in the AMN, mainly in the temperature of formation of the oxide. The SEM studies reveal that the crystallites and the agglomerates are different when the precursor is the metal nitrate or the metal chloride. The reacting media also influence the morphology of the oxide powders. On the whole, molten KNO_3 leads to the most significant modifications in crystal shape, size and their distribution. This feature cannot be attributed to the temperature of reaction, which is higher in KNO_3 than in the other AMNs. This high temperature, observed with the metal nitrates, is typical of the reaction of metal chlorides whatever the alkali metal nitrate.

Overall, these results show that when using molten salts synthesis for metal oxides for catalytic or sintering purposes, it is worth taking into account the initial experimental conditions. Some ions not specifically involved in the chemical process can have a direct influence on the morphology of the powder.

References

[1] D.H. Kerridge, in: J.J. Lagowski (Ed.), The Chemistry of Non-Aqueous Solvents, vol. VB, Academic Press, New York, 1978(Chapter 5).
[2] E.I. Eweka, D.H. Kerridge, Thermochim. Acta 290 (1996) 133–138.
[3] N.B. Singh, S.P. Pandey, Thermochem. Acta 67 (1983) 147–156.
[4] D.H. Kerridge, J. Cancela, Rey, J. Inorg. Nucl. Chem. 37 (1975) 975–978.
[5] D.H. Kerridge, S.A. Tariq, Inorg. Chem. Acta 4 (4) (1970).
[6] J.P. Deloume, J.P. Scharff, P. Marote, B. Durand, A. Abou-Jalil, J. Mater. Chem. 9 (1999) 107–110.
[7] M. Jebrouni, B. Durand, M. Roubin, Ann. Chim. Fr. 16 (1991) 569–579.
[8] A. Benamira, J.P. Deloume, B. Durand, J. Mater. Chem. 9 (1999) 2656–2662.
[9] K.H. Stern, J. Phys. Ref. Data 1 (1972) 747–772.
[10] P. Marote, B. Durand, J.P. Deloume, J. Solid Stat. Chem. 163 (2002).
[11] P. Marote, Thesis in Chemistry, Université Claude Bernard Lyon1, no. 161/2001 (2001).
[12] S. Gordon, C. Campbell, Anal. Chem. 27 (1955) 1102.
[13] W.W. Wendlandt, Tex. J. Sci. 10 (1958) 392.
[14] M. Le Van, Bull. Soc. Chim. Fr. 3 (1964) 545.
[15] J. Labat, Ann. Chim. 9 (7/8) (1964) 399.
[16] D. Weigel, B. Imelik, P. Lafitte, Bull. Soc. Chim. Fr. 544 (1962).
[17] P. Lumme, J. Peltonen, Suomen Kemistilehti 37B (9) (1964) 162.
[18] G. Le Van My, P. Perinet, Bianco, J. Chim. Phys. 63 (5) (1966) 719.
[19] R. Perrot, Bull. Soc. Chim. Fr. 2 (1966) 755.
[20] J. McDonald, H.T. Davis, J. Phys. Chem. 74 (4) (1970) 725–730.
[21] C.H. Liu, J. Hasson, G.P. Smith, Inorg. Chem. 7 (11) (1968) 2244–2247.